Supplemental Materials

Online Supplemental Methods

Mice

C57BL/6 and *Apoe*$^{-/-}$ mice were obtained from Jackson Labs. *Ccr5*$^{-/-}$*Apoe*$^{-/-}$ mice were provided by Dr. Weber Christian (Institute for Cardiovascular Prevention, Ludwig-Maximilians-University Munich, 80336 Munich, Germany). *CD45.1Apoe*$^{-/-}$ and *dsRed Apoe*$^{-/-}$ mice were generated by cross breeding *Apoe*$^{-/-}$ mice with *CD45.1* mice or *dsRed* mice (all purchased from Jackson Labs). *FoxP3GFPApoe*$^{-/-}$ mice were provided by Dr. Catherine Hedrick (La Jolla Institute, USA). All mice were on a C57BL/6 background. At 8 weeks of age, female and male *Apoe*$^{-/-}$ and B6 mice were fed with WD (TD.88137, Harlan). After 12 weeks to 20 weeks of WD feeding, the mice were used for flow cytometry. Mice were kept in an AAALAC-approved barrier facility under specific pathogen-free conditions. All mice were genotyped using standard PCR protocols (Transnetyx).

Aortic single-cell preparation

Mice were sacrificed by CO_2, and aortas were perfused with PBS containing heparin (20 U/ml). Aortas or carotid arteries were isolated by removal of all adventitial fat or surrounding muscles, cut into small pieces, and incubated for 50 to 60 minutes at 37°C with gentle shaking in a mixture of 237 U/ml collagenase type I, 190 U/ml collagenase type XI, 120 U/ml hyaluronidase, and 120 U/ml DNase I (all enzymes from Sigma-Aldrich) in HBSS.

Flow cytometry analysis

Cell suspensions were filtered through 70-μm cell strainers and stained with anti-mouse CD45-PerCP (clone 30-F11; BD Biosciences), anti-mouse TCRβ Alexa Flour 700 (clone H57-597; Biolegend), anti-mouse CD8 APC-Cy7 (clone 53-6.7; Biolegend), anti-mouse FoxP3 eF450 (clone FJK-16s ; eBioscience), antimouse IFN-γ PE-Cy7 (clone XMG1.2; BD Bioscience), anti-mouse T-bet APC (clone 4B10; Biolegend), anti-mouse CD25 APC (clone PC61.5; eBioscience), anti-mouse CD44 eF450 (clone IM7; eBioscience), anti-mouse CD62L PE-Cy7 (clone MEL-14; Biolegend), anti-mouse CCR5 PE (clone HM-CCR5; Biolegend), anti-mouse CXCR3 PE-Cy7 (clone CXCR3-173; Biolegend), anti-mouse CCR6 FITC (clone 221002; R&D) and LIVE/DEAD® Fixable Aqua Dead Cell Stain Kit (Life Technologies). For intracellular staining, FoxP3 staining buffer set (eBioscience) was used.

Quantification of atherosclerosis, histology and immunofluorescence

Isolated whole aortas were fix with 4% PFA and stained with Sudan IV. Digital images were obtained and analyzed by ImageJ to calculate the percentage of plaque area per aorta. Aortic roots were frozen in OCT compound on dry ice and stored at -80°C. 5-μm sections were taken in the aortic valve plane. Frozen sections were thawed and fixed for 10 minutes in isopropanol on ice. Sections were blocked by 10% normal goat serum (Sigma, G9023-10ML) for 1 hour at room temperature and then stained by rat anti-mouse CCR5-FITC (clone: HEK/1/85a; abcam) and rabbit anti-mouse CD3 (clone: ab5690; abcam), or by rabbit anti-mouse CCL5 (clone R6G9; eBioscience) and rat anti-mouse CD31-APC (clone MEC 13.3; BD Bioscience) over night followed by staining with secondary antibody: anti-FITC Alexa Fluor 488 (Molecular Probes) and anti-rabbit IgG Alexa Flour 650 (Abcam) or by anti-rabbit IgG Alexa Flour 568 (invitrogen). Images were acquired on a Leica DM6000 upright microscope using HCX PLAPO ×20 and ×40 oil-immersion objectives. Co-localization of fluorescence signal from CCR5 and CD3 was analyzed by ImageJ. In order to analyze co-localization, background was substracted from the CD3 and CCR5 channels. Then a CD3 mask channel showing only CD3 positive cells was created. Based on the mask a new CD3 and CCR5 channels which contained signal only within the masked area was created.

Cell sorting
For in vitro T cell homing assay, lymphocytes harvested from spleen were purified by RoboSep CD4 T cell negative selection (StemCell Technology). The effector ($CD4^+CD25^-CD44^{hi}CD62L^-$) and naïve ($CD4^+CD25^-CD44^{lo}CD62L^+$) T cells were stained with anti-mouse CD4 PE (clone rm4-5; Biolegend), anti-mouse CD25 APC (clone PC61.5; eBioscience), anti-mouse CD44 eF450 (clone IM7; eBioscience) and anti-mouse CD62L PE-Cy7 (clone MEL-14; Biolegend) and then sorted on FACSAria (BD Bioscience).

2 photon imaging
2-photon imaging was performed using a DM 6000 upright microscope with 4 nondescanned detectors (Leica Microsystems) and a Chameleon Ultra Ti: Sapphire laser (Coherent) tuned at 900–1,000 nm for acquisition using a water-dipping objective (Olympus XLUMPLFL 20XW, NA0.95). Emitted fluorescence was split with 2 dichroic mirrors (560 nm and 593 nm) and passed through filters (Semrock) at 535/22 nm, 585/40 nm, and 624/40 nm. Typically, 10–20 z planes spaced 10–15 µm apart were acquired at 512 × 512 pixels every 1 minute. Images were smoothed by median filtering at kernel size 3 × 3 pixels. 3D reconstructions of aortas were performed using Imaris software (version 7.1.1 ×64; Bitplane AG) after stitching several z series encompassing the artery using XuvTools software.

Treg suppression assay
To analyze CCR5Teff cell function, we performed a suppression assay with T cells derived from the para-aortic LNs of *FoxP3GFPApoe*$^{-/-}$ mice on WD >5 month. Splenic CellTrace Violet labeled $CD4^+CD25^-$ ($1x10^4$) T cells isolated from *Apoe*$^{-/-}$ mice on CD were cultured with a-CD3 mAb (1µg/ml) in the presence of $5x10^4$ irradiated (3000 Gy) T-depleted splenic APCs and decreasing amounts of $CD4^+CCR5^+$ cells or $CD4^+CCR5^-GFP^+$ conventional Tregs (at indicated ratio) sorted from para-aortic LNs of *Apoe*$^{-/-}$Foxp3GFP mice on WD > 5 mth. CellTrace Violet labeled $CD4^+CD25^-$ T cells were also cultured with $CD4^+CD25^+$ splenic conventional Tregs from *Apoe*$^{-/-}$CD mice or without Tregs as controls. After 4 days of culture in complete RPMI 1640 medium containing 10% FBS, penicillin/streptomycin, l-glutamine, NEAA, HEPES, and sodium pyruvate in 96-well round-bottom plates at 37°C and 5% CO2 in a humidified incubator, proliferation was measured by CellTrace Violet signal using flow cytometry, and supernatant was collected to measure cytokine secretion by mouse Th1/Th2/Th17 cytometric bead array (BD Biosciences).

In vivo T cell functional assay
CCR5Teff ($CD4^+CD25^-CCR5^+$) were sorted from the paLNs of *Cd45.1 Apoe*$^{-/-}$ mice on WD for > 5 months. $2x10^5$ CCR5Teff cells or saline were injected retro-orbitally into *Ccr5*$^{-/-}$*Apoe*$^{-/-}$ mice on WD for 2 months. Recipient mice were continued on WD for 12 weeks and sacrificed. Whole aortas were isolated, fixed with 4% PFA and stained with Sudan IV. Plaque area was quantified by imageJ.

Adoptive transfer
CCR5Teff ($CD4^+CD25^-CCR5^+$) cells, Treg ($CD4^+CD25^+CCR5^-$) and Teff ($CD4^+CD25^-CCR5^-CD44^{hi}CD62L^-$) were sorted from pooled paLNs from *Cd45.1Apoe*$^{-/-}$ mice on WD for 5 months. $2x10^5$ cells or saline were injected retro-orbitally into *Ccr5*$^{-/-}$*Apoe*$^{-/-}$ mice that have been on WD for 2 months. The recipient mice were kept on WD for 12 weeks before scarification.

Cytokine bead array

CCR5Teff ($CD4^+CD25^-CCR5^+$), Treg ($CD4^+CD25^+$) and Teff ($CD4^+CD25^-CCR5^-CD44^{hi}CD62L^{lo}$) were sorted from pooled paLNs from 5 *Apoe*$^{-/-}$ on WD for 5 month. Cells were cultured in complete RPMI 1640 media containing 10% FBS, penicillin/streptomycin, l-glutamine, NEAA, HEPES, and sodium pyruvate in the presence of cell stimulation cocktail (eBioscience) over night. Supernatants were collected and cytokine secretion was measured by mouse Th1/Th2/Th17 cytometric bead array (BD Biosciences).

RNA sequencing

CCR5Teff ($CD4^+CD25^-CCR5^+$), Treg ($CD4^+CD25^+$) and Teff ($CD4^+CD25^-CCR5^-CD44^{hi}CD62L^{lo}$) were sorted from pooled paLNs from 5 *Apoe*$^{-/-}$ on WD for 5 months. RNA was extracted from sorted cells using RNeasy micro kit (Qiagen). RNA quality was determined by bioanalyzer. RNA was reverse transcribed and tagged using the Nextera kit and RNA sequencing is performed on Illumina Hiseq 2500 using rapid run mode following SMARTseq II protocol from Illumina [66].

RNA sequencing data analysis. The single-end reads that passed Illumina filters were filtered for reads aligning to tRNA, rRNA, adapter sequences, and spike-in controls. The reads were then aligned to UCSC mm9 reference genome using TopHat (v 1.4.1) [67]. DUST scores were calculated with PRINSEQ Lite (v 0.20.3)[68] and low-complexity reads (DUST > 4) were removed from the BAM files. The alignment results were parsed via the SAMtools [69] to generate SAM files. Read counts of each genomic feature were obtained with the htseq-count program (v 0.6.0)[70] using the "union" option. After removing absent features (zero counts in all samples), the raw counts were then imported to R/Bioconductor package DESeq2[71] to identify differentially expressed genes among samples. DESeq2 normalizes counts by dividing each column of the count table (samples) by the size factor of this column. The size factor is calculated by dividing the samples by geometric means of gene counts (nth root of the product of gene counts across samples). This normalizes the counts being averaged, so that no counts dominate the weighting. P-values for differential expression were calculated using binomial test for differences between the base means of two conditions. These p-values were then adjusted for multiple test correction using the Benjamini Hochberg algorithm[72] to control the false discovery rate. We considered genes differentially expressed between two groups of samples when the DESeq2 analysis resulted in an adjusted P-value of <0.01. Cluster analyses including principal component analysis (PCA) and hierarchical clustering were performed using standard algorithms and metrics. Hierarchical clustering was performed using complete linkage with Euclidean metric. The sequences and reads counts used in this article have been submitted to the Gene Expression Omnibus under accession number XXXX (http://www.ncbi.nlm.nih.gov/geo/).

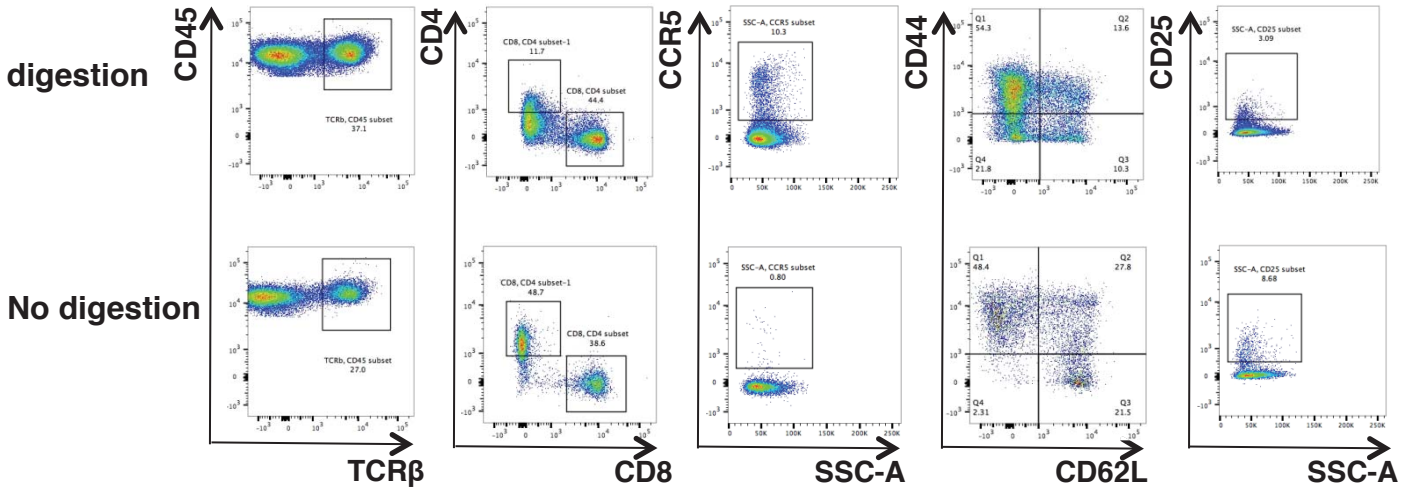

Online Figure I. **Digestion process affects surface expression of CD4, CCR5 and CD62L.** PaLNs were harvested from *Apoe*$^{-/-}$ mice fed on WD>5mth. Single cell suspension were split into two tubes. One was digested by enzyme cocktail as described in methods section. The other one was not digested. Cells were analyzed by multi-color flow cytometry. The populations shown in the figure are all gated on live singlets CD45^{+} cells.

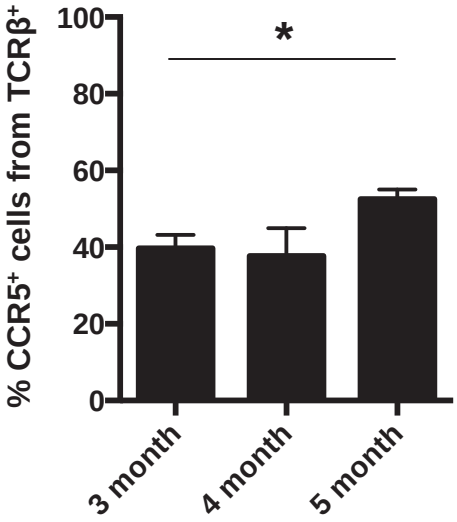

Online Figure II. CCR5 expression on T cells peaks at 5 month on WD in the aorta of *Apoe*$^{-/-}$ mice. Aortas from *Apoe*$^{-/-}$ WD mice (n=5 in each group) were harvested at different time point. Aortas were digested and the cells were analyzed by multi-color flow cytometry. The populations shown in the figure are gated on live CD45^{+}TCRb^{+}CD11b^{-} T cells. Gatings are set based on FMO controls and isotype controls. Values are mean ±SE. * $p<0.05$ 5month vs. 3 month, n=5, T-Test.

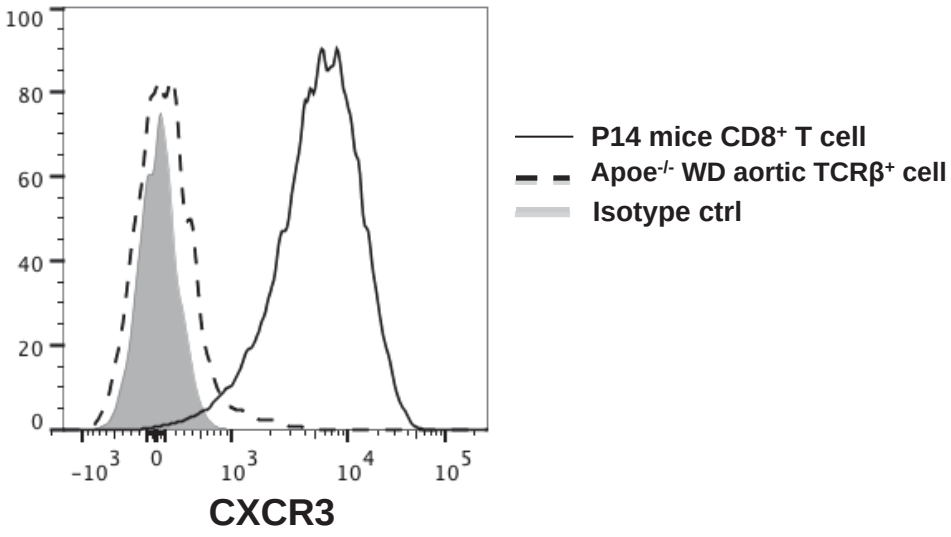

Online Figure III. CD8$^+$ T cells from P14 mice stimulated *in vitro* express CXCR3. CD8$^+$ T cells from p14 mice (transgenic mice of which the T cells recognize a peptide derived from lymphocytic choriomeningitis virus) were cultured in vitro with 10 U/ml rhIL2 for 6 days. Single cells suspension were stained by CXCR3 antibody or isotype antibody. Aortic single cell suspension from Apoe$^{-/-}$ WD mice was stained with the same CXCR3 antibody. The stained cells were analyzed by multi-color flow cytometry.

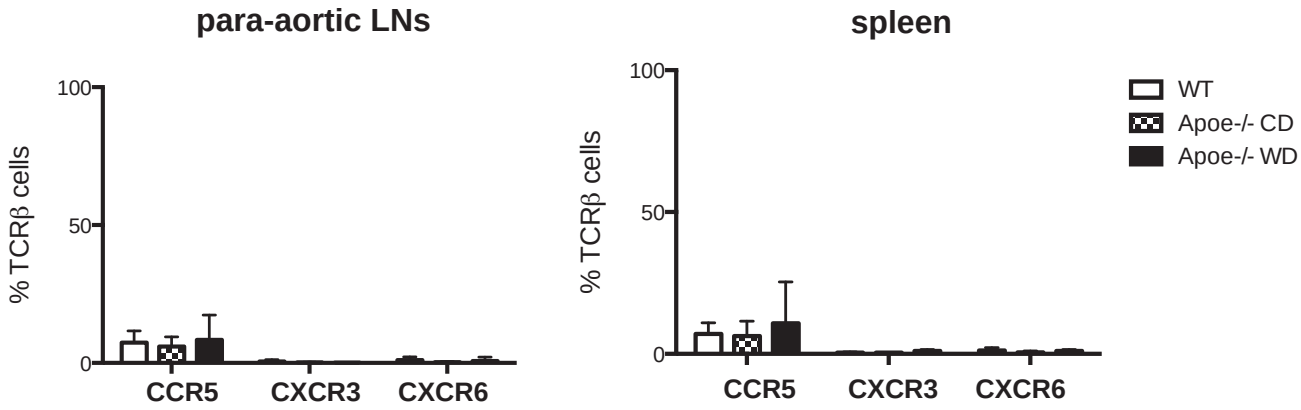

Online Figure IV. CCR5 or CXCR6 expression on T cells is not increased in the paLNs or spleen of *Apoe*$^{-/-}$ WD mice. paLNs and spleens from *Apoe*$^{-/-}$ WD mice, *Apoe*$^{-/-}$ CD mice and C56BL/6 WT mice (n=5 in each group) were harvested and the cells were analyzed by multi-color flow cytometry. The populations shown in the figure are gated on live CD45^{+}TCRb^{+}CD11b^{-} T cells. Gatings are set based on FMO controls and isotype controls. Values are mean±SD. * $p<0.05$ T-Test.

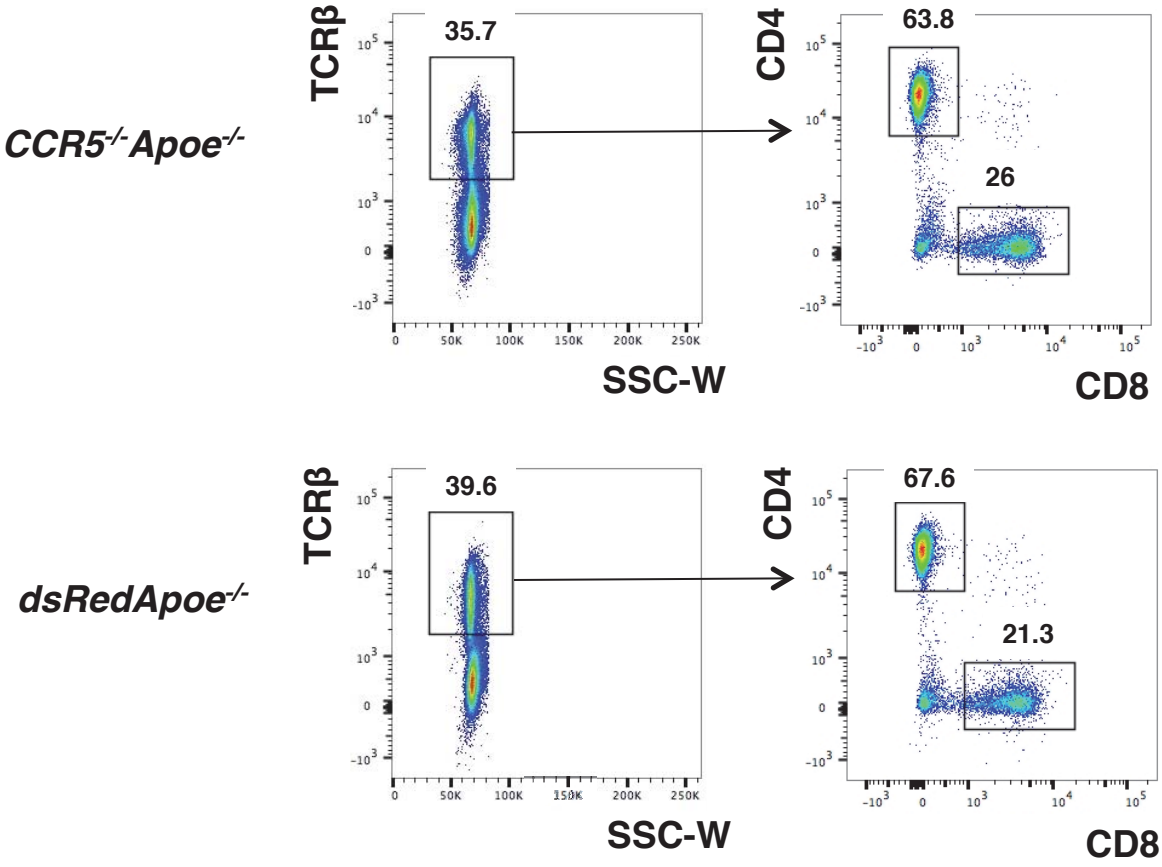

Online Figure V. Splenic T cell populations in *CCR5$^{-/-}$Apoe$^{-/-}$* mice are similar to *deRedApoe$^{-/-}$* mice. Splenocytes from *CCR5$^{-/-}$Apoe$^{-/-}$* and *dsRedApoe$^{-/-}$* mice fed on WD for 5 months were analyzed by flow cytometry. The populations shown are gated on live singlets CD45^{+} cells.

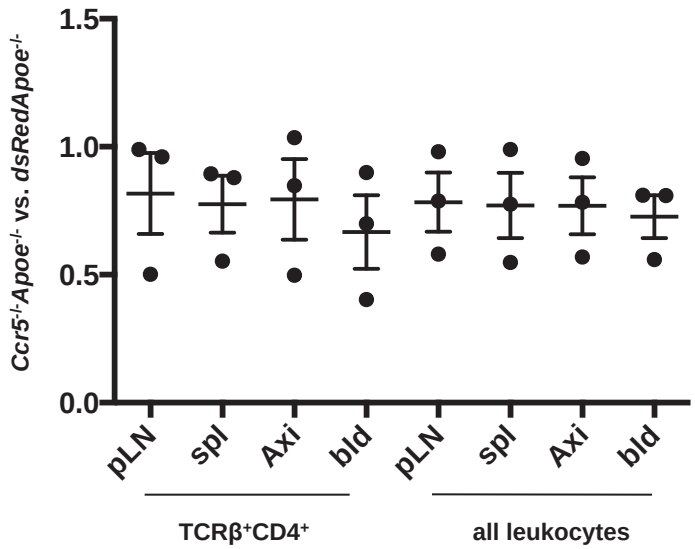

Online Figure VI. CCR5 deficient T cells efficiently homing to the lymphoid organs and blood in *Apoe*$^{-/-}$ WD mice. Totally 60x10^6 splenocytes from *dsRedApoe*$^{-/-}$ mouse and *Ccr5*$^{-/-}$*Apoe*$^{-/-}$ mouse at 1:1 ratio were adoptively transferred to *CD45.1Apoe*$^{-/-}$ WD mouse by retro-orbital injection. 24 hrs after transfer, the recipient mouse was sacrificed. Para-aortic LNs (pLN), spleen (spl), axillary LN (Axi) and blood (bld) were harvested and the cells were analyzed by flow cytometry. CD45.2 cells were gated from live, singlets, CD45.2$^+$CD45.1$^-$. The percentage of transferred TCRβ$^+$CD4$^+$ T cells and all CD45.2 leukocytes is normalized by its percentage in the input. Data shown is the fold change of *Ccr5*$^{-/-}$*Apoe*$^{-/-}$ vs. *dsRedApoe*$^{-/-}$. * p<0.05, t-test.

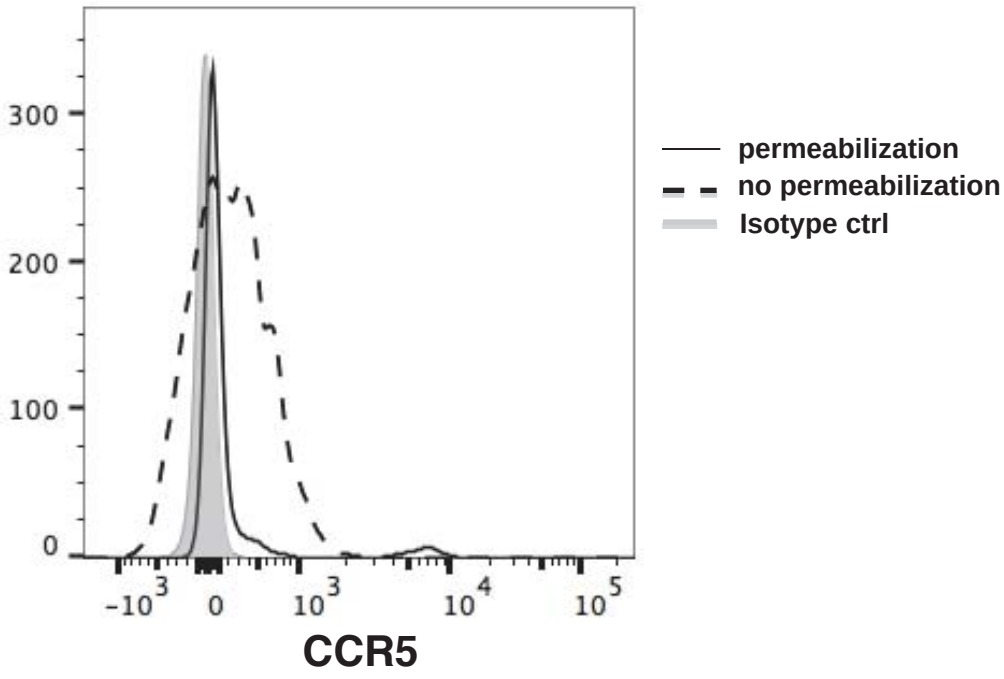

Online Figure VII . Permeabilization decreases CCR5 staining on T cells in the aorta of Apoe$^{-/-}$ mice on WD for 5. Aortas were harvested from *Apoe*$^{-/-}$ mice fed on WD for 5mth and digested as described in methods. Single cell suspension were stained with antibodies against surface antigens including CCR5 and followed by permeabilization or not. Cells were analyzed by multi-color flow cytometry. The populations shown in the figure are all gated on live singlets CD45^{+} TCRβ^{+}cells.

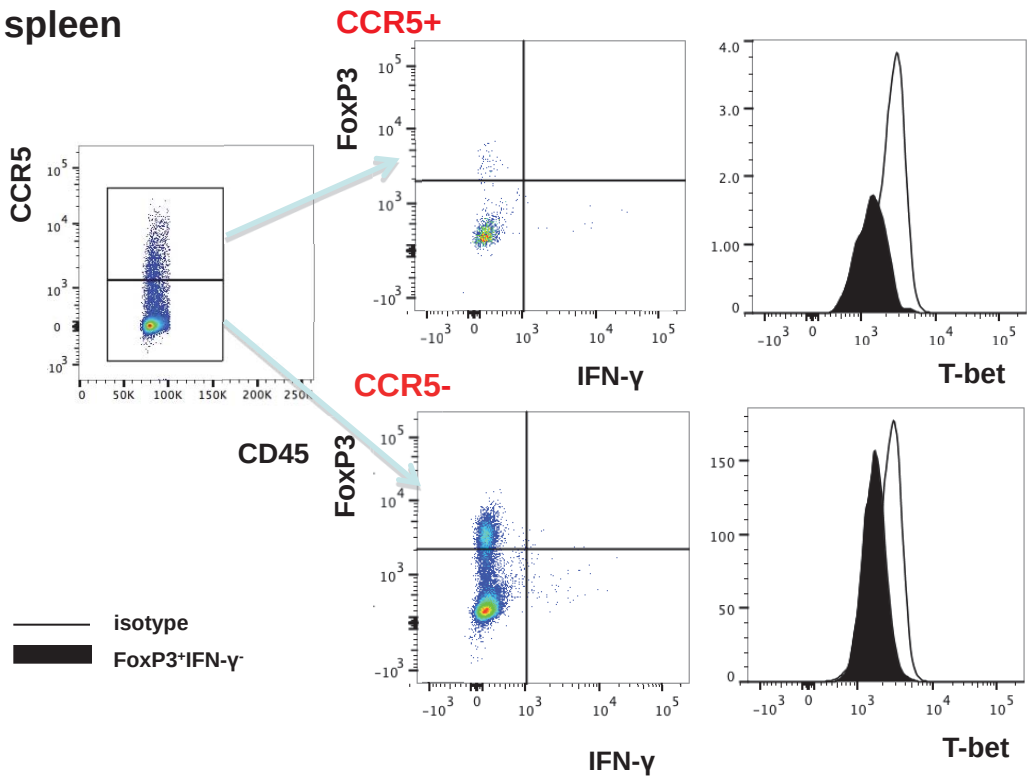

Online Figure VIII. **CCR5Teff cells are not present in the spleen of *Apoe*$^{-/-}$ WD mice.** Spleens were harvested from *Apoe*$^{-/-}$ WD mice. Single cell suspension from spleen were analyzed by multi-color flow cytometry. The populations shown in the figure are all gated on live CD45^{+} siglets TCRβ^{+} T cells. Gatings are set based on FMO controls and isotype controls. One representative experiment is shown.

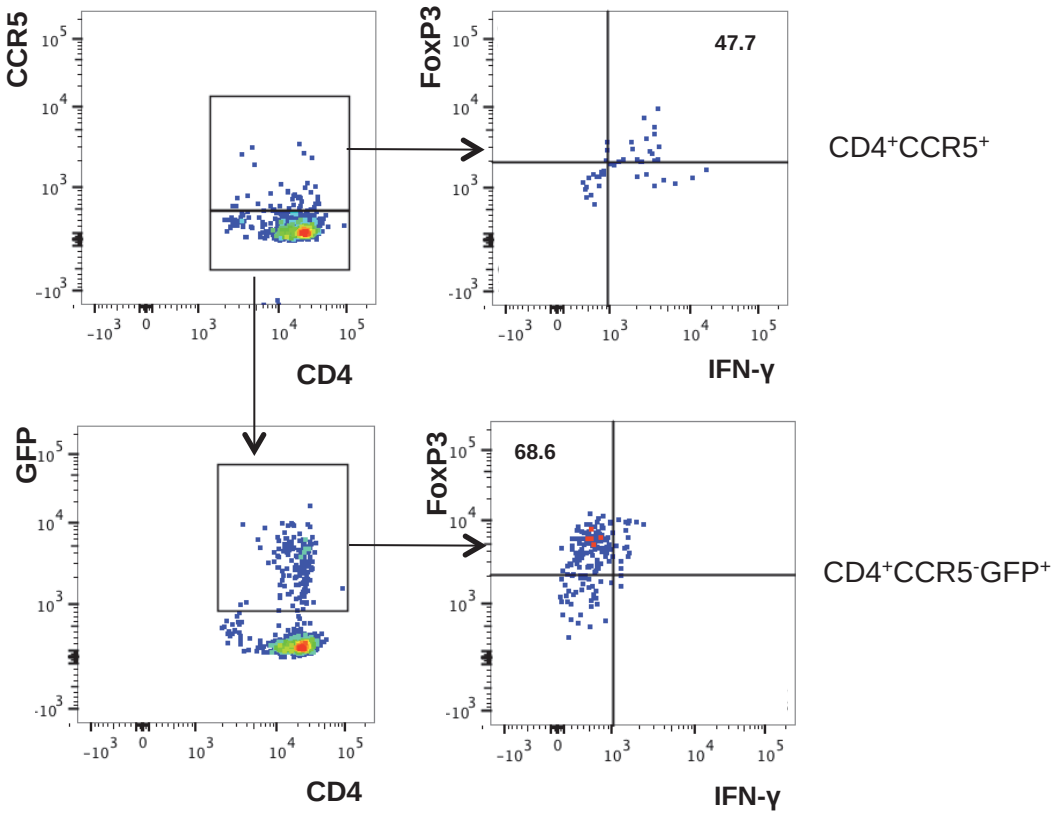

Online Figure IX. **Conventional Tregs and FoxP3^{+}IFN-γ^{+} cells from the paLNs of *FoxP3GFPApoe$^{-/-}$* WD mice.** PaLNs were harvested from *FoxP3GFPApoe$^{-/-}$* mice on WD>5mth. Single cell suspension from paLNs were analyzed by multi-color flow cytometry. The populations shown in the figure are all gated on live singlets CD45^{+} CD4^{+} T cells. Cells from CD4^{+}CCR5^{+} are mostly FoxP3^{+}IFN-γ^{+} cells. Cells from CD4^{+}CCR5^{-}GFP^{+} are mostly FoxP3^{+}IFN-γ^{-} conventional Tregs.

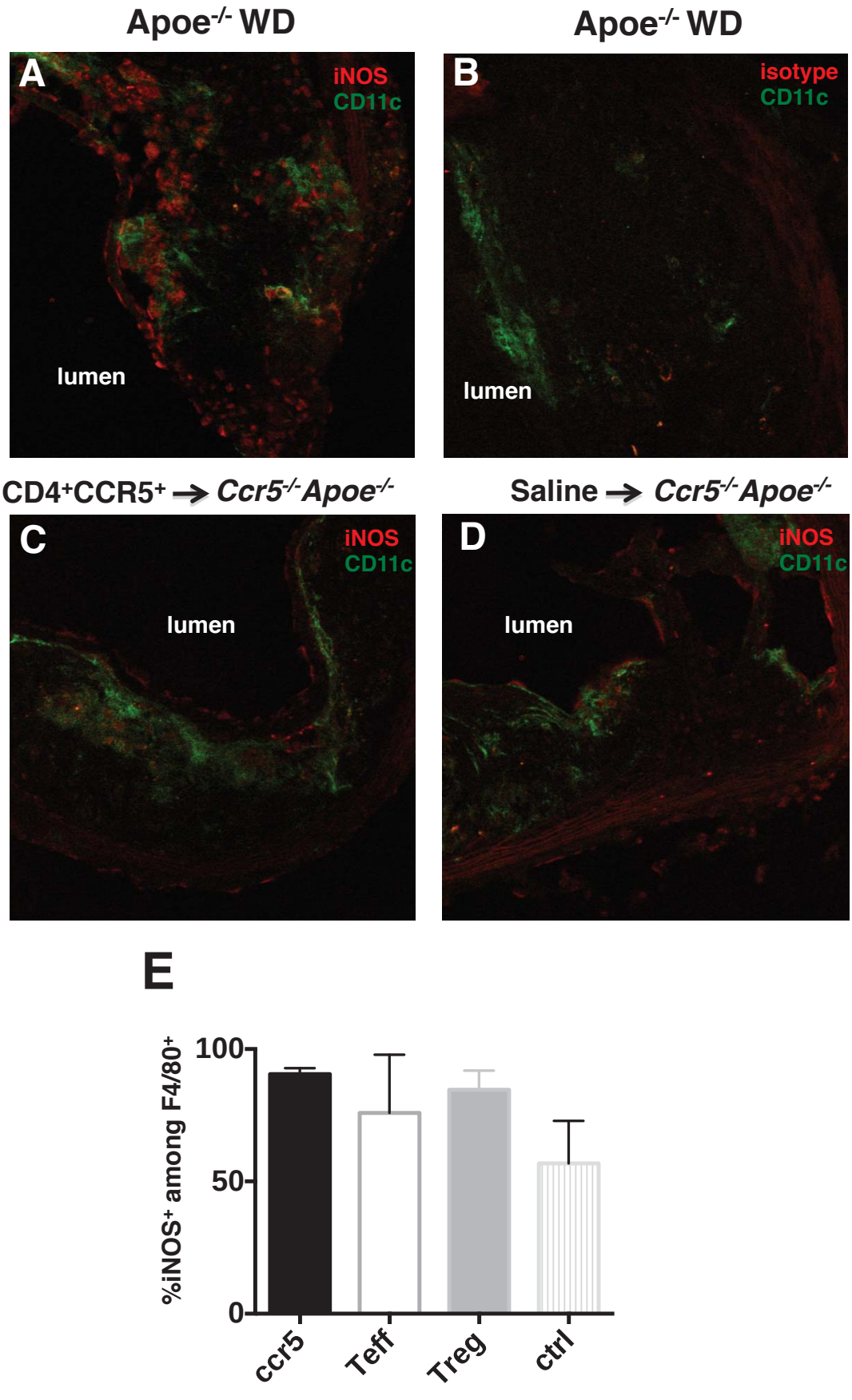
Apoe-/- WD
Apoe-/- WD
A
iNOS
CD11c
lumen
B
isotype
CD11c
lumen
CD4+CCR5+ → Ccr5-/-Apoe-/-
Saline → Ccr5-/-Apoe-/-
C
iNOS
CD11c
lumen
D
iNOS
CD11c
lumen
E
%iNOS+ among F4/80+
100
50
0
ccr5
Teff
Treg
ctrl

Online Figure X. **CCR5^{+}CD4^{+} T cells do not increase iNOS in the aorta of *Apoe*$^{-/-}$ mice.** Fresh frozen aortic root sections from **A** and **B**, *Apoe*$^{-/-}$ WD mice **C**, *Ccr5*$^{-/-}$*Apoe*$^{-/-}$ mice that transferred with 2x10^{5} CCR5^{+}CD4^{+} T cells or **D**, saline from Figure 7 were fixed and stained with fluorescently labeled antibodies against iNOS (red) and CD11c (green). **E**, 2 x 10^{5} CCR5Teff (CD4^{+}CCR5^{+}), Treg (CD4^{+}CCR5^{-}CD25^{+}), or Teff (CD4^{+}CCR5^{-}CD25^{-} CD44^{hi}CD62L^{-}) sorted from paLNs were cultured with explanted aorta from Apoe$^{-/-}$ CD mice over night. iNOS+ from F4/80+ cells were quantified by flow cytometry. Cells were gated on CD45+live singlets F4/80+ iNOS+. n=5.

Online Table

CCR5Teff vs. Teff

Gene	log2FoldChange	p value
Satb1	2.46	5.00E-14
Ccr7	1.79	7.90E-10
Ggt5	2.05	1.50E-08
Sell	1.9	8.50E-08
Gm14085	1.83	7.10E-06
Ampd1	1.75	1.50E-05
2610019F03F	1.51	0.00027
Pdlim4	1.6	0.00034
Treml2	1.45	0.001
Adh1	1.45	0.003
Cyp2d22	1.42	0.0044
Slc16a5	1.38	0.0062
Gpr146	1.29	0.0068
Tet1	1.29	0.0089
Ncr1	1.26	0.0092
Gm11346	1.09	0.0097
Als2cl	1.16	0.013
Pole2	1.27	0.016
Gabrr2	1.25	0.02
Ly6c1	1.12	0.023
Actn1	1.19	0.042
Fbxo17	1.06	0.05
Nedd4l	1.18	0.05

CCR5Teff vs. Treg

Gene	log2FoldChange	p value
Gbp1	-4.36	2.70E-34
Foxp3	-3	6.60E-29
Pltp	3.88	2.10E-23
Gata1	-2.83	2.10E-20
Klrg1	-2.94	5.90E-18
Padi4	3.38	6.50E-18
Gpm6b	2.44	1.40E-17
Gsta4	-3.2	3.00E-17
Lair1	2.87	5.30E-17
Ascl2	3.6	1.00E-16
Gbp3	-2.07	5.90E-16
Gm4956	-3.19	1.90E-14
Slc16a5	2.33	2.30E-13
2210020M01	3.59	3.90E-13
Socs2	-2.83	4.80E-13
Matn2	-2.3	4.90E-13
Itgae	-2.49	9.00E-13
Clec12a	3.42	2.80E-12
Capn3	-2.08	2.90E-12
Gal	3.34	1.00E-11
Ly6c2	2.92	1.40E-11
Ccl5	2.75	1.50E-11
Slc35d1	-2.36	1.90E-11
Fgl2	-2.33	2.00E-11
Igf2r	-2.14	2.10E-11
Pld4	2.82	2.10E-11
Anxa2	2.16	2.70E-11
Gpr34	-2.37	6.30E-11
Eno3	-2.37	1.00E-10
Slc2a3	-2.17	1.00E-10
Ifngr1	-1.78	1.60E-10
Atp1a3	2.81	2.80E-10
Dnahc7b	-3.09	8.80E-10
Syp	-2.69	9.40E-10
Themis	2.11	2.50E-09
Klra17	3.08	3.20E-09
Cd163l1	-3.07	4.20E-09
Angptl2	2.03	4.40E-09
Rgs1	-1.76	5.30E-09
Slc26a11	1.99	5.40E-09
Esm1	2.92	5.40E-09
Rnase6	2.46	5.40E-09
Epcam	-2.14	1.10E-08
Paqr5	3	1.20E-08
Alox5ap	2.84	1.20E-08

CCR5Teff vs. Teff

Gene	log2FoldChange	p value

CCR5Teff vs. Treg

Gene	log2FoldChange	p value
Cxxc5	2.26	1.50E-08
Sytl3	2.18	2.20E-08
Gpr15	-2.05	2.30E-08
Laptm4b	-2.17	2.80E-08
Ift80	-1.74	4.00E-08
Kmo	2.56	4.20E-08
C3	2.56	4.20E-08
C630004H02	1.74	4.20E-08
Phtf2	-1.53	4.20E-08
Tyrobp	2.33	4.20E-08
Cacna1d	2.63	5.60E-08
Gbp10	-1.72	7.10E-08
Il2rb	-1.43	7.90E-08
Pdcd1	1.69	7.90E-08
Spns3	2.72	1.40E-07
Atp1b1	1.58	1.60E-07
Galnt9	1.96	1.60E-07
Gsn	1.49	1.70E-07
BC013712	2.38	2.40E-07
Xkrx	2.25	2.60E-07
Cpne7	2.46	2.80E-07
Il21	2.66	2.80E-07
Sema4a	1.92	2.90E-07
Upb1	2.75	3.10E-07
Igfbp4	2.17	3.80E-07
Dap	1.48	4.00E-07
Gzma	2.51	4.00E-07
Gbp6	-1.41	4.10E-07
Rnf128	1.92	4.70E-07
Cd40lg	1.63	4.80E-07
Ccr5	2.25	5.70E-07
Abcc3	2.28	5.70E-07
Pde3b	2.37	5.70E-07
Ccr8	-1.62	6.50E-07
Cecr6	-2.65	6.60E-07
Smpdl3b	2.34	7.50E-07
Tox2	2.32	7.50E-07
Prg4	-2.06	7.50E-07
Plekho1	2.28	8.10E-07
Ispd	2.2	8.40E-07
Dntt	2.24	8.60E-07
H2-Q2	1.93	8.60E-07
Smtn	2.47	1.10E-06
Gpr83	-1.96	1.20E-06
Prss30	2.62	1.30E-06
Tcf7	1.41	1.60E-06
Evi2a	1.66	1.70E-06
Serpina9	2.15	1.70E-06

CCR5Teff vs. Teff

Gene	log2FoldChange	p value

CCR5Teff vs. Treg

Gene	log2FoldChange	p value
Samd3	1.94	1.90E-06
Gsto1	-1.81	2.50E-06
Cd86	-2.08	3.00E-06
Csf2rb	2.5	3.10E-06
AI836003	-2.53	4.40E-06
Dennd2d	1.54	4.80E-06
A430084P05	2.51	5.00E-06
Gm3002	-1.81	5.10E-06
Itgb1	1.48	5.10E-06
Tnfsf8	1.73	5.40E-06
Cd68	2.33	7.00E-06
Lcn10	-2.48	7.10E-06
Mctp2	1.97	8.50E-06
Ppic	1.86	8.70E-06
Hs3st1	2.37	9.40E-06
Hpcal1	1.46	9.40E-06
Mcoln2	1.94	1.10E-05
Slc22a2	-2.42	1.20E-05
Cd300c	2.42	1.30E-05
Smap2	1.41	1.30E-05
6330406I15R	-2.41	1.40E-05
Myo1e	-1.34	1.40E-05
Susd2	1.62	2.00E-05
Ceacam1	2.38	2.00E-05
Ehd3	1.21	2.20E-05
Ikzf4	-1.61	2.20E-05
Rcn1	-1.42	2.40E-05
Mettl9	1.56	2.40E-05
Epha3	2.36	2.60E-05
Sccpdh	1.71	2.80E-05
Slc22a5	-1.41	2.90E-05
1190002H23	1.56	3.00E-05
Lypd6b	2.15	2.90E-05
2610019F03I	1.89	3.30E-05
Tnc	2.32	3.40E-05
Lefty1	2.33	3.50E-05
Lyst	1.84	3.80E-05
Coro2b	1.78	3.90E-05
Ctla4	-1.28	3.90E-05
St6galnac1	2.29	4.70E-05
Ctsh	1.98	5.30E-05
Als2cl	1.5	6.60E-05
Slamf9	2.27	6.70E-05
Tmie	1.49	6.90E-05
Myc	-1.13	7.20E-05
Csgalnact1	1.78	7.80E-05
Cd300lf	2.13	8.30E-05
Kcnk1	-2.24	8.00E-05

CCR5Teff vs. Teff

Gene	log2FoldChange	p value

CCR5Teff vs. Treg

Gene	log2FoldChange	p value
Irak3	-1.58	0.00011
Tmem38b	1.39	1.00E-04
Ahcyl2	-1.55	0.00012
Dgat2	-1.79	0.00014
Enpp2	2.1	0.00014
Ptpra	1.25	0.00014
Efhd2	1.36	0.00015
Pkib	2.1	0.00016
Mboat1	1.39	0.00016
Sp6	-1.55	0.00016
Dnase1l3	1.92	0.00017
Gtf2i	1.14	0.00018
A530064D06	2.16	0.00019
2810474O19	-1.32	0.00019
Snord35b	1.56	0.00019
Asb2	1.39	0.00019
Grn	1.38	0.00019
St3gal6	1.67	2.00E-04
Crtam	1.76	0.00025
Syne2	1.37	0.00025
Apoc4	2.11	0.00026
Gbp2	-1.29	0.00026
Penk	-1.34	0.00026
Tnfaip8	1.08	0.00026
Vipr1	1.96	0.00026
Phlpp1	-1.67	0.00027
Rln3	-1.71	0.00028
S1pr2	1.2	0.00031
Krt17	1.89	0.00031
Rcan1	1.98	0.00034
Itih5	-1.47	0.00034
Gm2663	2.01	0.00035
H2-Aa	1.52	0.00036
Slc37a2	1.69	0.00036
6330512M04	2.03	4.00E-04
Plek	1.73	0.00041
Fcgrt	2.06	0.00042
Chn2	1.45	0.00044
Stx11	1.16	0.00044
Pros1	-1.61	0.00046
Tgfbr3	1.61	0.00046
Gm4951	-1.42	0.00049
Litaf	1.18	0.00049
Sytl1	-1.27	0.00049
Cfp	1.9	0.00051
Gramd1a	1.3	0.00051
Chchd10	-1.2	0.00053
A130040M12	1.68	0.00056

CCR5Teff vs. Teff

Gene	log2FoldChange	p value

CCR5Teff vs. Treg

Gene	log2FoldChange	p value
Cxcr5	1.12	0.00058
She	-1.6	0.00058
Tbc1d8	2.03	0.00057
App	2.01	0.00058
Lclat1	-1.33	6.00E-04
Gm12250	-1.11	0.00065
Ccl4	1.64	0.00071
Lyz2	1.6	0.00071
Baiap3	1.28	0.00074
Cd300a	1.98	0.00073
Cela1	1.84	0.00073
Gpr183	1.01	0.00078
Popdc2	1.96	0.00077
Apol9b	-1.64	0.00083
Il4	1.99	0.00082
Acpl2	1.51	0.00091
Axl	-1.35	0.00095
Ccdc28b	1.36	0.001
Nab1	1.07	0.001
Pfn2	1.37	0.001
Sfpi1	1.85	0.001
Itgad	1.95	0.0011
Swap70	-1.44	0.0011
Iigp1	-1.07	0.0011
Skil	-1.14	0.0011
Il12rb2	1.94	0.0012
Pgam2	1.91	0.0012
Socs1	-1.18	0.0012
Tlr7	-1.31	0.0012
Lax1	0.94	0.0013
Ccnd1	1.92	0.0013
Cd24a	1.93	0.0013
Sesn1	-1.11	0.0013
Cebpa	1.86	0.0013
Glipr2	-0.99	0.0013
Slamf6	1.07	0.0013
Gm11346	1.1	0.0015
5031414D18	1.86	0.0015
Mef2b	1.87	0.0015
Klhl4	1.91	0.0016
Tspan5	1.78	0.0016
Nod1	-1.12	0.0018
Idh2	0.99	0.0019
Il1rl1	-1.86	0.0021
Tifab	1.87	0.0021
Racgap1	1.09	0.0021
Tmsb10	-1.12	0.0021
Cnot6l	1.03	0.0022

CCR5Teff vs. Teff

Gene	log2FoldChange	p value

CCR5Teff vs. Treg

Gene	log2FoldChange	p value
Mpa2l	-0.97	0.0021
Adam8	-1.52	0.0022
Dopey2	1.22	0.0022
Nudcd1	-1.15	0.0022
Ppm1j	-0.98	0.0022
Cdc25b	1.06	0.0022
Sbk2	1.83	0.0022
Samhd1	-1.05	0.0023
Sdc4	-1.32	0.0025
Ccl3	1.83	0.0025
Dapl1	1.55	0.0025
Entpd1	-1.23	0.0026
BC026585	-1.57	0.0027
Slc9a9	1.2	0.0028
Ak8	1.81	0.0028
Bmyc	-1.34	0.0028
Ica1l	1.83	0.0029
Tns1	-1.52	0.003
B3gnt8	1.74	0.003
Ptrh1	1.49	0.0031
Rdx	-0.88	0.0031
Spib	1.48	0.0032
Suox	-1.07	0.0031
Mtrr	-1.03	0.0032
Anxa3	1.79	0.0032
H2-Q1	1.76	0.0032
Mtm1	-1.2	0.0032
Podnl1	1.09	0.0034
Zswim4	1.6	0.0034
Frmd6	-1.23	0.0035
4833442J19F	-1.41	0.0038
A330049M08	-1.37	0.004
Ifng	1.43	0.0042
Irak2	-0.96	0.0044
Lrrc66	-1.74	0.0042
Notch2	-1.3	0.0043
Smc4	-0.87	0.0042
Sykb	1.58	0.0042
Tgif1	-0.98	0.0042
Chd7	1.24	0.0045
Cybasc3	1.26	0.0047
Gfpt2	-1.77	0.0047
Gm10406	-1.55	0.0046
Snx13	-1.05	0.0047
Zfp36l1	-1.13	0.0046
C1qtnf6	-1.76	0.0048
Cdca7	-1.05	0.0049
Ly6a	0.93	0.0049

CCR5Teff vs. Teff

Gene	log2FoldChange	p value

CCR5Teff vs. Treg

Gene	log2FoldChange	p value
Slc1a4	1.76	0.005
Kirrel3	1.75	0.0051
Arglu1	-1.21	0.0054
Casp4	1.02	0.0054
Grtp1	1.74	0.0054
Hopx	-1.44	0.0054
Pak6	1.71	0.0056
Vdr	1.73	0.0054
Bcl11a	1.6	0.0056
Npepl1	1.09	0.0057
Il1rl2	1.63	0.006
Ly6d	1.47	0.0061
Ppm1l	-1.55	0.006
Rnd3	1.71	0.0059
Aldh3b1	1.72	0.0065
Cdh5	1.69	0.0064
Tgfbr1	-1.02	0.0064
Sgk1	1.45	0.0068
AF251705	1.67	0.0069
Irf8	1.03	0.007
Ncoa7	-0.99	0.0069
Chad	-1.67	0.0073
Reep1	1.7	0.0073
Rpia	1.7	0.0073
Trp53i11	-0.87	0.0073
Tspan2	1.7	0.0071
Cd22	1.06	0.0075
Gpr137b	1.66	0.008
H2-Eb1	1.21	0.0079
A830080D01	-1	0.008
Afp	1.38	0.008
Sirpa	1.67	0.008
Gas7	1.63	0.0087
Mfge8	1.1	0.0087
Atp2a1	1.67	0.0091
Jun	-1.36	0.0089
Ubqln4	-1.08	0.0089
H2-Ab1	1.43	0.0096
Il9r	1.34	0.0096
Optn	1.55	0.01
Abcb1a	-0.92	0.011
Akap12	1.22	0.011
1700019D03	1.44	0.011
Lgals3	1.33	0.011
Fam20a	1.62	0.012
Paqr7	1.24	0.011
Cnksr3	-1.49	0.012
Shmt1	-1.06	0.012

CCR5Teff vs. Teff

Gene	log2FoldChange	p value

CCR5Teff vs. Treg

Gene	log2FoldChange	p value
Hspa2	1.59	0.012
Lsm7	-0.94	0.012
Lyz1	1.31	0.013
Stk11	1.25	0.013
Dusp6	1.02	0.013
Fam43a	1.41	0.013
Nkg7	1.27	0.014
Arhgap18	-0.92	0.014
Heyl	1.55	0.014
Tmem136	-1.49	0.014
Plaur	1.42	0.014
Abi3bp	-1.56	0.014
Amigo2	1.61	0.014
Hras1	1.6	0.015
1700001O22	1.54	0.015
Gzmm	1.61	0.015
Mcat	1.38	0.015
Ebi3	-1.11	0.015
Pcsk4	-1.39	0.015
Vill	-1.19	0.016
Lag3	0.94	0.016
Exoc4	0.91	0.016
Rara	-0.94	0.017
Fam169b	-0.75	0.017
Galnt2	1.3	0.018
Igtp	-0.91	0.018
Napsa	1.4	0.018
Snn	1.41	0.018
Siah1a	1.44	0.019
Adam11	1.5	0.019
Dmd	-1.52	0.019
H2-DMb1	1.36	0.019
Rnf125	1.03	0.019
Itgax	1.56	0.019
Kcnip2	-1.38	0.019
Ly86	1.38	0.019
Ampd1	1.52	0.019
Adh1	1.2	0.019
Egln3	1.25	0.02
Stat1	-0.94	0.02
Traf3ip2	0.82	0.02
Wdr82	-0.97	0.02
Msra	0.87	0.02
Ndrg4	1.56	0.02
Pim1	-1.23	0.02
Wdr26	0.9	0.021
Arrdc4	-1.26	0.022
Spin2	-1.14	0.022

CCR5Teff vs. Teff

Gene	log2FoldChange	p value

CCR5Teff vs. Treg

Gene	log2FoldChange	p value
Stx1a	-1.16	0.022
Eepd1	1.51	0.022
Fads3	1.5	0.022
Psap	0.8	0.022
Scamp1	-1.52	0.022
Cd5l	1.53	0.023
Fasl	1.14	0.023
Tnfrsf9	-0.96	0.023
Gpr155	0.97	0.023
Rasgrf1	1.5	0.023
Ramp3	1.18	0.024
Dusp4	-1.19	0.024
Zeb2	1.52	0.024
Gna13	1.1	0.025
Il3ra	-1.08	0.025
Mctp1	-1.19	0.025
Cxcr3	0.87	0.026
Plcg2	1.27	0.026
Tmem221	1.48	0.026
Gna14	1.31	0.026
Lysmd2	-1.28	0.026
Stt3b	1.16	0.026
2310004I24R	0.91	0.027
Acsbg1	-1.12	0.026
Cbfa2t3	1.5	0.027
Ptpro	1.43	0.027
2010001M0	1.41	0.029
Ccr6	-1.35	0.028
Ccrl2	-0.99	0.028
Dok2	-0.87	0.027
Lrba	1.34	0.028
Pole2	1.17	0.028
Rad51c	1.5	0.028
Rnf145	0.87	0.028
Slamf7	1.11	0.028
Tsc22d1	1.18	0.028
Acadsb	-0.89	0.031
Ifnar1	-0.76	0.031
Klk1b27	1.49	0.03
Lef1	0.9	0.03
Mfsd6	1.42	0.03
Pip5k1b	-1.48	0.031
Pipox	1.48	0.031
Pla2g2d	1.36	0.03
Prf1	0.94	0.029
Tmem149	-0.86	0.031
2210010C17I	-0.78	0.033
I830077J02R	1.47	0.033

CCR5Teff vs. Teff

Gene	log2FoldChange	p value

CCR5Teff vs. Treg

Gene	log2FoldChange	p value
Klrd1	1.47	0.031
Nmral1	1.21	0.033
2310015A10	-1.02	0.034
Ccdc120	1.44	0.034
Fads2	1.39	NA
Fyn	0.92	0.035
N6amt2	-0.89	0.034
Nacc2	1.41	0.034
Bcl6	1.12	0.037
Gbp4	-0.82	0.037
Il4ra	-0.99	0.037
Mmp9	-1.46	0.035
Plscr4	1.46	0.036
Rgmb	1.44	0.036
Ryr1	1.4	0.037
Stk32c	1.39	0.037
Tnfrsf18	-0.93	0.037
Fbln2	-1.41	0.037
Mgst2	-0.96	0.039
Mthfd1	-0.81	0.038
Rps6kl1	1.44	0.038
Src	-1.45	0.038
Camkk1	-1.12	0.04
Casp1	0.79	0.04
Cyp39a1	1.44	0.039
Phxr4	1.44	0.04
Sh3bp5	-0.79	0.04
X99384	1.36	0.039
Abat	-1.43	0.042
AI480653	-1.09	0.042
Ccnb1	1.05	0.041
Cyp2s1	1.31	0.042
Obscn	1.37	0.041
Rbpj	-0.9	0.042
Tdpoz4	-1.41	0.042
4930524L23F	-1.42	0.044
Atp8b4	1.35	0.044
Kif22	1.15	0.044
Nvl	-0.79	0.043
Zfml	-1.01	0.043
Abcb9	0.74	0.045
Slc20a1	0.9	0.045
Tbx21	1.01	0.045
Tnks	1.2	0.044
Btla	0.8	0.047
Car5b	1.37	0.047
Gm14446	-0.75	0.048
Kit	-1.32	0.047

CCR5Teff vs. Teff

Gene	log2FoldChange	p value

CCR5Teff vs. Treg

Gene	log2FoldChange	p value
Rasip1	-1.36	0.047
Slc35f2	-1.01	0.048
Capg	-1.02	0.049
Magi1	-1.31	0.049
Stc2	1.37	0.048
Trak1	1.15	0.049
Unc93b1	0.97	0.049
Zadh2	1.08	0.049
Zbtb32	1.02	0.048
Zdhhc20	-0.67	0.049